

**AD-A188 337**

**REPORT DOCUMENTATION PAGE**

**DTIC FILE COPY**

UNCLASSIFIED		1b. RESTRICTIVE MARKINGS	
2a. SECURITY CLASSIFICATION AUTHORITY		3. DISTRIBUTION/AVAILABILITY OF REPORT	
2b. DECLASSIFICATION/DOWNGRADING SCHEDULE		Approved for public release; distribution unlimited.	
3. PERFORMING ORGANIZATION REPORT NUMBER(S)		5. MONITORING ORGANIZATION REPORT NUMBER(S)	
N/A			
6a. NAME OF PERFORMING ORGANIZATION	6b. OFFICE SYMBOL (if applicable)	7a. NAME OF MONITORING ORGANIZATION	
Naval Weapons Center			
6c. ADDRESS (City, State, and ZIP Code)		7b. ADDRESS (City, State, and ZIP Code)	
China Lake, CA 93555-6001			
8a. NAME OF FUNDING/SPONSORING ORGANIZATION	8b. OFFICE SYMBOL (if applicable)	9. PROCUREMENT INSTRUMENT IDENTIFICATION NUMBER	
Office of Naval Research			
8c. ADDRESS (City, State, and ZIP Code)		10. SOURCE OF FUNDING NUMBERS	
Arlington, VA 22217		PROGRAM ELEMENT NO. 61153N	PROJECT NO. RR01301
		TASK NO. RR01301	WORK UNIT ACCESSION NO. 138540
11. TITLE (Include Security Classification)			
FTIR and FTNMR Study of Organophosphorus Surface Reactions			
12. PERSONAL AUTHOR(S)			
Melvin P. Nadler, Robin A. Nissan, and Richard A. Hollins			
13a. TYPE OF REPORT	13b. TIME COVERED	14. DATE OF REPORT (Year, Month, Day)	15. PAGE COUNT
End of Year	FROM 86 Oct TO 87 Sep		
16. SUPPLEMENTARY NOTATION			
For Submission to Applied Spectroscopy			
17. COSATI CODES		18. SUBJECT TERMS (Continue on reverse if necessary and identify by block number)	
FIELD	GROUP	SUB-GROUP	
19. ABSTRACT (Continue on reverse if necessary and identify by block number)			
See attached			
20. DISTRIBUTION/AVAILABILITY OF ABSTRACT		21. ABSTRACT SECURITY CLASSIFICATION	
<input checked="" type="checkbox"/> UNCLASSIFIED/UNLIMITED <input type="checkbox"/> SAME AS RPT. <input type="checkbox"/> DTIC USERS		UNCLASSIFIED	
22a. NAME OF RESPONSIBLE INDIVIDUAL		22b. TELEPHONE (Include Area Code)	22c. OFFICE SYMBOL
Melvin P. Nadler		619-939-1610	3851

**DTIC**  
**SELECTED**  
**NOV 23 1987**  
**S & D**

FTIR AND FTNMR STUDY OF ORGANOPHOSPHORUS SURFACE REACTIONS

Melvin P. Nadler, Robin A. Nissan, and Richard A. Hollins

Chemistry Division, Research Department

Naval Weapons Center, China Lake, CA 93555-6001

↓

Fourier transform infrared (FTIR) and Fourier transform nuclear magnetic resonance (FTNMR) methods were used to examine the adsorption and reaction of diisopropyl fluorophosphate (DFP) on various solid adsorbents. Static and flow system experiments were monitored using FTIR to determine DFP adsorption rates and isotherms on silica, coated silicas, <sup>g. m. m.</sup> alumina, coated aluminas, and activated charcoal. The adsorption of DFP(3) onto the solid adsorbents was generally very rapid, with a half-life of 20 seconds for 1 mg DFP onto 25 mg of 350 <sup>g. m.</sup> m<sup>2</sup>/g silica. The DFP adsorption isotherms on silica indicated chemisorption to a monolayer at P/P<sub>0</sub> < 0.6, followed by increased coverage that appears to be physical adsorption. Diffuse reflectance infrared Fourier transform (DRIFT) spectroscopy, photoacoustic spectroscopy (PAS), and solid state <sup>31</sup>P NMR of adsorbed DFP showed chemisorption on silica and on alumina. Bonding at the P=O of DFP was indicated by a -41/cm<sup>-1</sup> shift in the <sup>ν</sup>(P=O) and a 1 ppm upfield shift in the <sup>(31)</sup>P resonance. DRIFT, PAS kinetics and <sup>31</sup>P NMR showed that DFP hydrolyzed after the initial adsorption on alumina and some coated materials but not on silica or activated charcoal. The rate of hydrolysis increased on alumina with addition of water and varied with different aluminas and coated silicas.

## INTRODUCTION

The decomposition of DFP and other toxic organophosphorus compounds by hydrolysis or other methods is of interest because of their severe environmental and personnel hazards. Current disposal methods require the use of toxic and/or corrosive materials and protection methods are only temporary. Adsorption by activated charcoal does not chemically change the adsorbate, making disposal difficult, and when the surface is saturated breakthrough occurs, followed by loss of protection. An ideal technique would consist of rapid removal from the environment and then catalytic decomposition of the toxic organophosphorus compound.

Posner et al.<sup>1</sup> reported that  $\gamma$ -alumina can accelerate the hydrolysis of acyl and phosphoryl fluorides in diethyl ether solution. Recent work at this laboratory has shown that in water/t-butanol solution alumina and silica supported species can increase the hydrolysis rate of DFP and p-nitrophenyl diphenylphosphate (NPDPP).<sup>2</sup> Kuiper et al.<sup>3</sup> investigated the hydrolysis of gaseous isopropylmethylphosphonofluoridate (IMPF) on  $\gamma$ -alumina by infrared (IR) transmittance. Templeton and Weinberg<sup>4</sup> examined gaseous dimethylmethylphosphate (DMMP) on alumina using inelastic tunneling spectroscopy. The latter two studies give surface structures for adsorbed species and possible mechanisms for the hydrolysis, but no kinetic information. Another paper by Kuiper et al.<sup>5</sup> uses a microcalorimetric method to obtain kinetic data on the surface reaction of IMPF with  $\gamma$ -alumina.

Our work will show that FTIR and FTNMR can give surface structure information for DFP on silica, alumina, and coated silica and alumina using

DRIFT, PAS, and  $^{31}\text{P}$  solid state NMR.<sup>5</sup> DRIFT and PAS can also give kinetic data on surface reactions. Adsorption isotherms and adsorption rates will also be discussed using FTIR to monitor the DFP under static and flow conditions.

### SPECTRAL ASSIGNMENTS FOR DFP

The IR and NMR spectra of DFP must be characterized and vibrational assignments made before realistic surface information can be obtained.

#### Infrared

Nicolet 7199 and 60SX FTIR spectrometers were used for the IR measurements, and the neat DFP (obtained from Aldrich Chemical) spectra were collected at  $1\text{ cm}^{-1}$  resolution. Figure 1 shows the fingerprint region for both gaseous and liquid DFP and Table I gives the vibrational frequencies and assignments. Most of the vibrational assignments were made from previous work on similar compounds<sup>3,7-14</sup> or from analysis of impurities in the DFP using gas chromatography (GC), GC-FTIR, and NMR. Gas chromatography of DFP using an XE-60 column on Anakrom Q showed three impurities. Isopropanol was observed at  $2 \pm 0.5\%$ , and two additional impurities of lower volatility than DFP at less than 5% were observed. GC-FTIR showed both of the impurities to have IR spectra similar to DFP(g), but the  $869\text{ cm}^{-1}$  band was missing, the  $\nu(\text{P}=\text{O})$  were shifted down to about  $1278\text{ cm}^{-1}$ , and  $\nu(\text{P})-\text{O}-\text{C}$  was at  $1011\text{ cm}^{-1}$  for the lower volatility impurity and  $979\text{ cm}^{-1}$  for the other. The lower volatility impurity is probably triisopropyl phosphate, and the other impurity is another alkyl



Dist	Special
A-1	

phosphate. Since  $\nu(\text{P-F})$  for  $(\text{CH}_3\text{O})_2\text{FPO}^{14}$  is at  $860\text{ cm}^{-1}$  and  $^{31}\text{P}$  NMR shows the two impurities to be nonfluorine containing compounds, the  $869\text{ cm}^{-1}$  band is assigned to  $\nu(\text{P-F})$ .

### Solution State NMR

NMR spectra were recorded on an NT-200 wide-bore spectrometer operating at 81 MHz for  $^{31}\text{P}$  and at 200 MHz for  $^1\text{H}$  acquisition. Solution state  $^{31}\text{P}$  spectra were recorded in  $\text{CDCl}_3$  and referenced to an external sample of 85%  $\text{H}_3\text{PO}_4$  at 0 ppm with chemical shifts upfield of the reference designated as negative.  $^1\text{H}$  spectra were recorded in  $\text{CDCl}_3$  and referenced to the residual  $\text{CHCl}_3$  peak at 7.26 ppm.

The solution state  $^{31}\text{P}$  NMR spectrum of DFP consists of a doublet centered at -10.1 ppm with  $J_{\text{P-F}} = 960\text{ Hz}$ .<sup>15,16</sup> Two other resonances were observed for as received DFP, at +6.0 and +9.8 ppm, that were assigned to impurities having no P-F coupling. These impurities were estimated at less than 5% from integration over the  $^{31}\text{P}$  spectrum. The  $^1\text{H}$  NMR spectra of fresh DFP showed the existence of 2% isopropanol. This was confirmed by addition of isopropanol to the DFP. A  $^{31}\text{P}$  NMR of a DFP residue (low volatility components have been concentrated) showed the expected DFP doublet, the +6.0 and +9.8 ppm resonances, and a new resonance centered at +1.0 ppm, which is tentatively assigned to diisopropylphosphate.

## STATIC INFRARED CELL ADSORPTION STUDY

### Experimental

A 10 cm IR cell with KBr windows and an extension for the solid adsorbent was used to examine DFP adsorption rates. The solid adsorbent was weighed, placed in the solid holder, then the IR cell was evacuated, and the stirrer started before a saturated DFP/N<sub>2</sub> mixture was added from a bulb. DFP disappearance was monitored using rapid scan (3-5 scans/s) FTIR just before DFP addition and during the initial stages of adsorption. Scans at longer time intervals were taken for the remainder of the process. The 1028 cm<sup>-1</sup> (P)-O-C stretch was used to monitor the DFP.

The time for DFP absorbance to reach a maximum was only one second after DFP addition, with no solid adsorbent present. The solid adsorbents used were not pretreated to simulate normal atmospheric conditions and the IR cell was always pressurized to 1 atm of saturated DFP in N<sub>2</sub>.

### Results

In general, the adsorption of gaseous DFP onto silica, activated charcoal, and surface-modified silicas is very rapid, with a half-life of 20 seconds for 1 mg DFP onto 25 mg of 350 m<sup>2</sup>/g silica (large pore--Strem Chemicals, Inc.). The DFP adsorption rate is a function of the particle size and weight

while the capacity is a function of surface area and surface structure. Figure 2 shows DFP adsorption rates and capacities for 5 mg of three different surface area silicas. Note that the lower surface area silicas limit the capacity of DFP adsorbed, but the rate of adsorption for the flamed silica (very fine silica) is higher than that for the higher surface area silica (350 m<sup>2</sup>/g). This is due to the smaller average particle size of the flamed silica. Table II shows quantitative DFP adsorption capacities for different silicas and Whetlerite activated charcoal calculated from limiting adsorption tests, such as 52 m<sup>2</sup>/g and flamed silica in Fig. 2. It should be noted that the DFP adsorption is not proportional to the Brunauer, Emmett, and Teller (B.E.T.) surface area and coated silicas have a lower capacity than uncoated silicas (Table II). The relative adsorption rates and capacities for three different charcoals are shown in Fig. 3. Both the Whetlerite and Grant charcoals are activated (i.e., porous), but the Grant charcoal had a much smaller average particle size and showed a faster adsorption rate. The Sterling R is a graphitized carbon black charcoal having no pores and showed almost no DFP adsorption.

Low capacity adsorption or slow adsorptions could not be measured because of a slow adsorption/reaction of DFP with the glass surfaces of the IR cell and/or the stopcock grease. This loss of DFP in an empty cell was only 5-10% for the first 1000 seconds and only had a minor effect on the faster adsorption phenomena. The static cell gave qualitative comparisons of adsorption rates and approximate DFP capacities (near saturation), but a more quantitative method was required to measure adsorption isotherms, the effect of added water, desorption products, and slower adsorption/reaction phenomena.

## FLOW SYSTEM STUDY

### Experimental

The flow system shown in Fig. 4 was used to obtain a constant partial pressure of DFP in  $N_2$  for determining adsorption isotherms of different solid adsorbents, with and without added water. FTIR was used to monitor the DFP level, in real-time, by collecting spectra at 0.5 to 2 minute intervals, processing and displaying each spectrum, and calculating the integrated absorbance of the (P)-O-C stretch at  $1028\text{ cm}^{-1}$ . The data collection and processing was performed using a MACRO, which is a subroutine written to do a specific sequence of FTIR instructions. When the desired absorbance (i.e.,  $P/P_0$ ) is reached, the DFP/ $N_2$  flow is diverted through the solid adsorbent by opening the two 3-way solenoids (see Fig. 4). For greater time resolution, the GC-FTIR software was used to obtain spectra at  $<1$  second intervals.

Figure 5 shows an integrated absorbance versus time plot of the DFP  $\nu((P)\text{-O-C})$  obtained from the spectral data using a kinetic analysis program written in compiled BASIC. The DFP level takes about 10 minutes to reach a constant absorbance and then at 15 minutes the DFP/ $N_2$  flow is diverted into the solid chamber containing 26 mg of  $350\text{ m}^2/\text{g}$  Strem silica. For this run the DFP was rapidly adsorbed and at about 23 minutes breakthrough occurred followed by a slow return to the original DFP absorbance level. Calibration of the DFP  $P/P_0$  versus integrated absorbance of the  $1028\text{ cm}^{-1}$   $\nu((P)\text{-O-C})$  from  $1070\text{-}985\text{ cm}^{-1}$  gave a linear plot of slope 1/8.0 for  $P/P_0$  greater than 0.05. If the data in Fig. 5 is replotted as  $A(\text{max})-A$  versus time, then the area under the curve from 14.8 to 51.3 minutes is proportional to the total DFP

adsorbed by the adsorbent. Using the vapor pressure of DFP at 20°C (0.579 mm),<sup>17</sup> the following equation was used to calculate the total mg of DFP adsorbed:

$$\text{Total mg DFP adsorbed} = \frac{162.4 F}{PT} \int_{t_1}^{t_2} A(1028) dt \quad (1)$$

F = total flow rate of DFP/N<sub>2</sub> in cc/min

P = total pressure in mm

T = temperature (K)

t<sub>1</sub> = onset of DFP adsorption (min)

t<sub>2</sub> = end of DFP adsorption (min)

A(1028) = integrated absorbance of DFP v((P)-O-C)

NOTE:  $\frac{A(1028)}{8.0} = \frac{P}{P_0}$  for DFP

This technique allows adsorption isotherms to be obtained by varying the F/P<sub>0</sub>.

The mg of DFP desorbed by N<sub>2</sub> can be determined at the end of an adsorption experiment by monitoring the DFP level when only N<sub>2</sub> is flowing through the solid chamber. A correction for wall desorption must be made at the same P/P<sub>0</sub> to obtain DFP desorbed from the solid adsorbent.

## Results

Figure 6 shows the adsorption isotherm for DFP on Strem 350  $m^2/g$  silica. The weight of DFP adsorbed quickly rises to a monolayer at about 0.22 (mg/mg silica), followed by increased coverage ( $P/P_0 > 0.6$ ) that appears to be physical adsorption. When water was added to the DFP/ $N_2$  at the 44% relative humidity level, the amount of DFP adsorbed was within experimental error of falling on the dry adsorption isotherm (see Fig. 6).

Coated silicas were also examined and Fig. 7 shows the adsorption isotherm for DFP on a silica-bound ethylenediamine (SiEDA). The coated silicas were prepared at this laboratory and details can be found in another publication.<sup>2</sup> Figure 7 shows a possible monolayer coverage at low  $P/P_0$ , but most of the DFP coverage appears to be physical adsorption. Again, when water was added at 46 and 93% relative humidity, only a slight increase in DFP adsorbed was observed. This increase is within experimental error as shown by the dotted isotherm in Fig. 7. A silica-bound diethylenetriamine (SiDETA) was examined at 48% relative humidity and again is within experimental error of falling on the dry SiEDA silica adsorption isotherm. The chemiadsorption of DFP at lower  $P/P_0$  is decreased by SiEDA coating (the coating uses active DFP sites), but at higher  $P/P_0$  the physical adsorption of DFP onto silica or coated silica is only slightly changed. Apparently, the presence of water does not effect the adsorption of DFP.

Figure 8 shows an example of  $N_2$  desorption of DFP from SiEDA silica, untreated silica, and the flow system walls at  $P/P_0 = 0.7 \pm 0.02$ . Calculations show that about 70% of the adsorbed DFP was removed from the SiEDA

silica and only 15% from the untreated silica. Desorption experiments with Whetlerite activated charcoal showed that less than 15% of the DFP was removed, indicating a strong physical adsorption.<sup>3</sup>

The flow system can also be used to monitor desorbed reaction products during an adsorption run by collecting spectra with the GC-FTIR software. In some adsorption experiments, isopropanol was observed (0-9 weight % of the total DFP adsorbed) when the DFP was at a minimum. Figure 9 shows three GC reconstructions of the spectral data from an adsorption experiment of DFP onto Woelm alumina. The 1070-985  $\text{cm}^{-1}$  reconstruct follows the  $\nu((\text{P})-\text{O}-\text{C})$  of DFP and shows that initially all DFP is adsorbed by the alumina, followed by a slow increase after 9.3 min to the original level. No clear isopropanol band could be found so a series of basis vectors for  $\text{H}_2\text{O}$ , background, and DFP were used to subtract from the Gram-Schmidt to follow isopropanol and  $\text{CO}_2$  (from air spike). Note that  $\text{H}_2\text{O}$  is first removed from the alumina followed by isopropanol and then the DFP comes back slowly to the initial  $P/P_0$  of the bubbler. It was shown that isopropanol was an impurity in the DFP at about the 2% level and since it is more volatile than DFP a larger fraction adsorbs onto the solid with a shorter retention time. Successive DFP adsorption tests showed that isopropanol decreased and finally could not be observed. Water and  $\text{CO}_2$  were observed at  $\ll 1\%$  from trapped air and/or the solid surface. In conclusion no desorbed reaction products could be detected. The next section will discuss FTIR and FTNMR methods that allow observation of surface species and surface reactions and will aid in clarifying some of the static cell and flow system results.

## SURFACE REACTIONS

### Experimental

The static cell and flow system experiments only measure the change in gas phase DFP concentration as the result of adsorption and/or reaction on the surface of an adsorbent, but DRIFT and PAS permit examination of surface species by interpretation of their IR spectra. Harrick (on 7199) and Barnes (on 60SX) diffuse reflectance cells were used to obtain FTIR spectra at  $4\text{ cm}^{-1}$  resolution of final adsorption/reaction products and an MTEC model 100 PA cell (on 60SX) was used to obtain spectra at  $8\text{ cm}^{-1}$  resolution as a function of time for DFP on various solid adsorbents. DRIFT could not be used for kinetics due to DFP adsorption onto the transparent matrix of KBr, KCl, or Si. However, DRIFT gives superior signal/noise and time resolution for samples that would not adsorb or redistribute onto the transparent matrix. The MTEC PA cell with the Nicolet 60SX gives good signal/noise with only 50-100 scans at VEL = 50-70 and total scan times of only 25-60 seconds.

Samples were prepared either by adding 2-5  $\mu\text{L}$  of DFP(l) to 150 mg of the solid adsorbent (with or without 2-4  $\mu\text{L}$   $\text{H}_2\text{O}$ (l)) or using the flow system to adsorb DFP(g) (+  $\text{H}_2\text{O}$ (g) in some cases) at a fixed P/P<sub>0</sub>. The samples were given at least 24 hours to react and then mixed with KBr to obtain the DRIFT spectra of the final products. For PAS kinetic runs the samples were prepared with the flow system and immediately transferred into the PA cell. DFP addition had to be optimized to prevent any gaseous DFP from entering the PA cell and yet obtain maximum surface coverage (i.e., 40-60% of a monolayer).

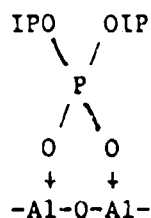
Solid state  $^{31}\text{P}$  NMR spectra were recorded on an NT-200WB spectrometer operating at 81 MHz with magic angle spinning<sup>18</sup> using a one pulse sequence with the experimental pulse width corresponding to a 45 degree pulse. Spectra were referenced to an external solution of 85%  $\text{H}_2\text{PO}_4$ . In general, to achieve a reasonable signal to noise, one thousand or more scans were required.

### DRIFT and PA Spectroscopy

Figure 10 shows DRIFT spectra of final (after 24 hours) DFP adsorption/reaction species on Woelm alumina (top trace) and Strem silica (middle trace) compared to a transmittance spectrum of liquid DFP. Table III gives the vibrational frequencies of the adsorbed/ reacted species on silica and alumina. Comparing the DFP +  $\text{H}_2\text{O}$  on silica with the liquid DFP frequencies in Table I shows good agreement except for the  $\nu(\text{P}=\text{O})$  at about  $1257\text{ cm}^{-1}$  (shifted  $-41\text{ cm}^{-1}$ ) and the  $\nu((\text{P})-\text{O}-\text{C})$  at  $1026\text{ cm}^{-1}$  (shifted  $+5\text{ cm}^{-1}$ ). There are other minor differences and some subtraction artifacts in the region of strong silica bands. The strong negative peak at  $3744\text{ cm}^{-1}$  indicates loss of free  $\text{Si}-\text{OH}$  or reaction with DFP. An increase in associated OH on the silica surface is indicated because of the strong broad band from about  $3450-3200\text{ cm}^{-1}$ . DFP must bond to the surface at the oxygen of the  $\text{P}=\text{O}$  because of the  $-41\text{ cm}^{-1}$  shift in the  $\nu(\text{P}=\text{O})$  for the adsorbed species. This is in agreement with Kuiper who reported a  $-35\text{ cm}^{-1}$  shift for the  $\nu(\text{P}=\text{O})$  of DFP and comparable shifts in other phosphates when adsorbed onto alumina.<sup>3</sup> The top spectrum in Fig. 10 shows some major changes in the spectrum of the adsorbed/ reacted species of DFP +  $\text{H}_2\text{O}$  on alumina

- (a) a strong broad band centered about  $1140\text{ cm}^{-1}$ , (assigned to  $\nu(\text{Al-F})$ ),<sup>3</sup>
- (b) no observable  $\nu(\text{P=O})$ ,
- (c) a new band at  $1082\text{ cm}^{-1}$  (assigned to  $\nu_s(\text{P}(\text{O})_2)$ )<sup>3,4</sup> and also  $1180\text{ cm}^{-1}$  (assigned to  $\nu_a(\text{P}(\text{O})_2)$ )<sup>3,4</sup> has increased in intensity compared to isopropyl vibrations,
- (d)  $\nu((\text{P})\text{-O-C})$  has shifted  $-10\text{ cm}^{-1}$ .

The above IR frequency changes observed for DFP on alumina are consistent with those observed by Kuiper<sup>3</sup> for IMPF on alumina and by Templeton<sup>4</sup> for DMMP on alumina. Assuming the same hydrolysis mechanism postulated by Kuiper<sup>3</sup> and Templeton<sup>4</sup> our IR results and the  $^{31}\text{P}$  NMR results showing loss of P-F bonds (see next section) indicate the following hydrolysis product for DFP on alumina



PAS was used to monitor the kinetics of the adsorption/reaction process on various solid adsorbents, since the samples could be run neat and no interfering transparent diluent (i.e., KBr, KCl, or Si) was required as in DRIFT. Figure 11 shows spectra at 8 - 123 minutes for the reaction of DFP on Alcoa CS3350 alumina. The PA spectra were taken at  $8\text{ cm}^{-1}$  resolution, 100 scans, VEL = 50 (Nicolet 60SX) and ratioed to a carbon background, then the PA spectrum of the Alcoa alumina was subtracted. The early spectrum at 8 minutes

(NOTE: This is initial scan since adsorption process required 8 minutes.) shows adsorbed DFP, with the  $\nu(\text{P}=\text{O})$  at  $1270\text{ cm}^{-1}$  and the  $\nu((\text{P})-\text{O}-\text{C})$  at  $1032\text{ cm}^{-1}$ , as well as, other adsorbed DFP vibrations shown in Table III. Note the weak band at about  $1000\text{ cm}^{-1}$ , which is the start of reacted or hydrolyzed  $\nu((\text{P})-\text{O}-\text{C})$  as can be seen in the final spectrum at 123 minutes. The final spectrum also shows no  $\nu(\text{P}-\text{O})$  or observable  $\nu(\text{P}=\text{F})$ .

The hydrolysis rates are shown in Figure 12 by following the normalized integrated absorbance of  $\nu(\text{P}=\text{O})$  adsorbed at  $1270\text{ cm}^{-1}$  referenced to the  $\delta(\text{CH}_3)$  versus time for two types of porous Alcoa alumina. The adsorbed  $\nu((\text{P})-\text{O}-\text{C})$  at  $1032\text{ cm}^{-1}$  gives the same rate of decrease as the  $\nu(\text{P}=\text{O})$  and the growth of hydrolysis product can be followed by using either  $\nu((\text{P})-\text{C}-\text{C})$  at  $999\text{ cm}^{-1}$  or  $\nu_s(\text{PO}_2)$  at  $1082\text{ cm}^{-1}$ , but the  $\nu(\text{P}-\text{F})$  at about  $870\text{ cm}^{-1}$  is too weak and in an area of poor signal/noise (See next section of  $^{31}\text{P}$  NMR for indication of P-F bond cleavage.). Both alumina samples were dried in a vacuum oven overnight at  $110^\circ\text{C}$  and then exposed to air at about 30% relative humidity before conducting the hydrolysis reactions. Note the time for complete hydrolysis of DFP on Alcoa CSS350 alumina is only 38 minutes ( $t_{1/2} \sim 13\text{ min}$ ) and almost 150 minutes ( $t_{1/2} \sim 25\text{ min}$ ) on Alcoa F200 alumina (Fig. 12). DFP has a 250 minute half-life on Woelm alumina which only has a B.E.T. surface area of  $100\text{ m}^2/\text{g}$  compared to  $600\text{ m}^2/\text{g}$  for the two Alcoa aluminas. If the alumina is saturated with water vapor prior to DFP addition, the rate of hydrolysis increases by about a factor of two (NOTE: This gives a  $t_{1/2}$  of  $\sim 5\text{ min}$  for CSS350 alumina.).

DFP hydrolysis was also examined on coated silicas (Strem-- $350\text{ m}^2/\text{g}$ ) and aluminas (Alcoa CSS350-- $600\text{ m}^2/\text{g}$ ) since previous work at this laboratory

showed that certain coated silicas increased the hydrolysis rate in water.<sup>2</sup> Photoacoustic kinetics showed that gaseous DFP hydrolyzed on three coated silicas (SiEDA, SiDE1A, and octadecyldimethyl[3-trimethoxysilyl]propyl]ammonium chloride (SiQOCT) that were saturated with H<sub>2</sub>O(g). However, the rate was quite slow, SiQOCT gave a DFP half-life of about 600 minutes by following the decrease in the adsorbed  $\nu((P)-O-C)$  at 1032 cm<sup>-1</sup>. Addition of liquid DFP to water saturated coated silicas gave ambiguous results due to the difficulty in completely distributing the DFP(l) onto the surface by mixing. In most cases hydrolysis occurred at a slower rate than gaseous addition ( $t_{1/2}$  -1200 min on SiQOCT) due to the slower adsorption and distribution of the DFP. Hydrolysis of DFP on coated aluminas occurred at a slower rate than on uncoated alumina due to a decrease in active sites.

### Solid State <sup>31</sup>P NMR

The substantial coupling constant ( $J_{P-F} = 960$  Hz) observed in the solution state <sup>31</sup>P spectrum offers us a unique method for monitoring phosphorus-fluorine bond cleavage on solid adsorbents and supported catalyst systems. Fig. 13 shows the <sup>31</sup>P spectrum of DFP on a silica surface. The <sup>31</sup>P resonance is centered at -11.5 ppm and the coupling constant  $J_{P-F} = 960$  Hz. This is very similar to the solution state spectrum of DFP in CDCl<sub>3</sub>, except for the broadness of the resonance (a consequence of solid state interactions) and a 1 ppm upfield shift. A silica sample, where treatment of the solid phase with water preceded addition of DFP, yielded an identical <sup>31</sup>P spectrum with no evidence for P-F bond cleavage (i.e., no DFP hydrolysis after 48 hours).

Various other solid adsorbents were tested with respect to their tendency to facilitate the hydrolysis of DFP. These materials included SiEDA, SiDETA, SiQOCT, alumina, and Whetlerite charcoal. Two typical solid state  $^{31}\text{P}$  NMR spectra illustrating the results obtained when hydrolysis occurs are shown in Fig. 14.

It is clear that DFP on SiDETA, SiEDA, or alumina undergoes hydrolysis within 24 hours. There is no evidence for any phosphorus compounds bearing a directly bound fluorine in these materials (see Figure 14b). However, given the relatively low signal to noise ratio in these spectra, we can only be confident in asserting that less than 10% of the fluorinated phosphate remains after 24 hours of reaction on these two surfaces. Addition of water to these three supports prior to adsorption of DFP had no influence on the outcome of the reactions after 24 hours. We observed one broad ( $\sim 1000$  Hz wide at half height) resonance centered at  $\sim -1$  ppm for each of these materials whether in the presence or absence of added water. The material SiQOCT was one example where intermediate stages of DFP hydrolysis could be observed in the solid state  $^{31}\text{P}$  NMR spectra. In the absence of added water, resonances expected for adsorbed DFP and a shoulder on the downfield side of the DFP were observed (Figure 14a). The shoulder appears near  $-1$  ppm and almost certainly represents some degree of P-F hydrolysis reaction. This is a reasonable observation since it was noted in the PAS studies that the half-life for DFP hydrolysis on SiQOCT is 20 hours. The  $^{31}\text{P}$  solid state NMR spectrum of DFP on SiQOCT with added water helps to verify this conclusion. Addition of water to this system leads to complete hydrolysis within 48 hours (Figure 14b). In this case, the observed resonance is centered at  $+2$  ppm, but once again, there was

no evidence for any remaining fluorophosphate type compounds. Finally, we examined the solid state  $^{31}\text{P}$  NMR of DFP on Whetlerite charcoal. The resonance observed was quite broad and centered at -15 ppm, however, the  $J_{\text{P-F}}$  coupling was still apparent (see Fig. 15). Addition of water led to further broadening of the resonance, but no evidence for P-F hydrolysis could be obtained. The upfield shift of this phosphorus resonance was attributed to a strong interaction between the DFP and the surface. Peak broadening can be attributed to the presence of paramagnetic metal ions used in the preparation of Whetlerite charcoal.

## CONCLUSIONS

FTIR and FTNMR are shown to be useful for examination of DFP adsorption and surface reactions on silica, coated silica, alumina, and activated charcoal. Adsorption rates can be followed using rapid scan FTIR and adsorption isotherms determined by quantitative IR measurements of DFP adsorbed in a flow system. Desorption products can also be monitored using GC-FTIR software. Surface species are examined using DRIFTS and solid state  $^{31}\text{P}$  NMR. Finally surface reactions can be followed (without a diluting matrix) using a sensitive photoacoustic cell combined with the ability of the FTIR to obtain good signal/noise PA spectra at  $8\text{ cm}^{-1}$  resolution in 25-60 seconds.

Heterogeneous reactions can be divided into five stages:

- (1) Diffusion of reactants to the surface,
- (2) Adsorption on the surface,
- (3) Chemical reaction at the surface,

- (4) Desorption from the surface, and
- (5) Diffusion of products away from the surface.

For gaseous reactants, diffusion to and from the surface is rapid [stage (1) and (5)], but for liquids the rate may be diffusion-controlled. Some of the discrepancies between solution<sup>1</sup> or slurry<sup>2</sup> results and gas-solid studies may be due to differences in the diffusion rate.

The adsorption rate of gaseous DFP (stage 2) onto solid adsorbents is faster than the surface reaction (stage 3) as long as there is an excess of total surface area available for DFP adsorption to a monolayer and the particle size is small (<100  $\mu$ ). The surface hydrolysis of DFP on water treated Alcoa CSS350 alumina has a half-life of only 5 minutes, which is still slower than the adsorption time of about 20 seconds for a 0.5 DFP monolayer. For most of the other solids tested, the adsorption rate was more than an order of magnitude faster than the surface reaction. The presence of adsorbed water had little effect on the DFP adsorption isotherms, therefore DFP adsorbs at different sites. Kuiper<sup>3</sup> also showed that pretreatment of alumina in vacuo at 900°C did not affect the adsorption of IMPF. However, the surface reaction of DFP was greatly affected by pretreatment with water, for Alcoa CSS350 alumina the hydrolysis rate increased by about a factor of two compared to untreated alumina.

DFP does not hydrolyze on silica or activated charcoal but does "strongly" adsorb. The adsorbed DFP bonds to the surface at the oxygen of the P=O; IR and NMR show the DFP molecules remain unchanged. Certain coated silicas, such as, SiEDA, SiDETA, and SiQOCT<sup>2</sup> hydrolyzed DFP at a slow rate

(600-1200 minute half-lives) with water pretreatment. Coated alumina hydrolyzed DFP slower than uncoated alumina, indicating that the coating only used up active sites and did not aid in the reaction.

Kuiper's explanation that a "basic" surface promotes hydrolysis<sup>3</sup> agrees with our results since alumina has more active basic sites than silica<sup>19</sup> and the active coatings used have basic sites.<sup>2</sup> Kuiper also shows that for  $\gamma$ -alumina 110 face, the Al-Al distance is the exact spacing for the oxygens of the POO group of the hydrolyzed IMPF.<sup>3</sup> Therefore, adsorbed DFP on alumina can readily lose HF by reaction with a surface -OH forming the POO group on the surface, however, on a silica surface the Si-Si distance makes this step unlikely and the adsorbed DFP remains.

#### ACKNOWLEDGMENT

This work was supported in part by the Office of Naval Research.

## REFERENCES

1. G. H. Posner, J. W. Ellis, and J. Ponton, *J. Fluor. Chem.* **19**, 191 (1981).
2. R. A. Hollins, "The Acceleration of Organophosphorus Ester Hydrolysis by Alumina and Silica-Supported Species," submitted to *J. Catalysis*.
3. A. E. T. Kuiper, J. J. G. M. van Bokhoven, and J. Medema, *J. Catalysis* **43**, 154 (1976).
4. M. K. Templeton and W. H. Weinberg, *J. Am. Chem. Soc.* **107**, 97 (1985).
5. J. J. G. M. van Bokhoven, A. E. T. Kuiper, and J. Medema, *J. Catalysis* **43**, 168 (1976).
6. C. A. Fyfe, *Solid State NMR for Chemists*, (C.F.C. Press, Guelph, Ontario, 1983).
7. R. A. Nyquist, *Appl. Spectrosc.* **4**, 161 (1957).
8. L. W. Daasch and D. C. Smith, *Anal. Chem.* **23** (6), 853 (1951).
9. J. G. David and H. E. Holliman, *J. Chem. Soc. (A)*, 1103 (1966).
10. L. C. Thomas and R. A. Chittenden, *Spectrochim. Acta* **20**, 467 (1964).
11. L. C. Thomas and R. A. Chittenden, *Spectrochim. Acta* **20**, 489 (1964).
12. G. G. Guilbault, E. Scheide, and J. Das, *Spectrosc. Lett.* **1** (4), 167 (1968).
13. F. S. Mortimer, *Spectrochim. Acta* **9**, 270 (1957).
14. D. E. C. Corbridge, *Topics in Phosphorus Chemistry*, Vol. 5, M. Grayson and E. J. Griffith, Eds. (John Wiley and Sons, Inc., New York, 1969), pp. 235-365.

15. Annual Reports on NMR Spectroscopy, E. F. Mooney, Ed.  
(Academic Press, New York, 1973).
16. R. Greenhalgh and M. A. Weinberger, *Can. J. Chem.* **45**, 495 (1967).
17. Aldrich Technical Information Bulletin Number AL-122, Aldrich Chemical Company, Inc., 1981.
18. E. R. Andrew, D. J. Bryant, E. M. Cashell, and B. A. Dunell, *Chem. Phys. Lett.* **77**, 614 (1981).
19. A. V. Kiselev and V. I. Lygin, Infrared Spectra of Surface Compounds  
(John Wiley and Sons, New York, 1975), p. 237.

TABLE I. Vibrational Frequencies ( $\text{cm}^{-1}$ ) for DFP.

Gas	Liquia	Assignment
2991	2986	$\nu_a(\text{CH}_3)$
2952	2940	$\nu_s(\text{CH}_3)$
2887	2881	$\nu(\text{CH})$
1473	1469	} $\delta_a(\text{CH}_3)$
1457	1457(sh)	
1389	1389	} $\delta_s(\text{CH}_3)$
---	1380	
---	1358(vw)	$\delta(\text{CH})$
1333(sh)	1304(sh)	---
1313(m)	1298(m)	$\nu(\text{P}=\text{O})$
---	1264(sh)	impurity band
1182	1181	$\text{CH}_3$ wag
1144	1145	$\nu_a(\text{C}-\text{C}-\text{C})$
1115	1108	$\nu(\text{O}-\text{C})$
1028(vs)	1021(vs)	$\nu((\text{P})-\text{O}-\text{C})$
---	939(vw)	---
913	901	$\text{CH}_3$ rock
869	861	$\nu(\text{P}-\text{F})$
786(vw)	780(w)	} $\nu(\text{P}-\text{O}-\text{C})$
757(w)	748(w)	
---	720(vw)	---
559	551	} P-O-C bends or 511 } may be P-F bend
511	511	
435	426	---

TABLE II. Amount of DFP Adsorbed Using Static Cell.

(Initial $P/P_0 = 1.0$ )	
Solid Adsorbent	mg DFP/mg solid
Silica (very fine-flame)	0.19
Silica ( $52 \text{ m}^2/\text{g}$ )*	0.15
Silica ( $350 \text{ m}^2/\text{g}$ )*	0.22
Silica coated with SiQOCT†	0.18
Whetlerite activated charcoal ( $1000 \text{ m}^2/\text{g}$ )*	0.50

\* B.E.T. surface area.

†  $350 \text{ m}^2/\text{g}$  coated with octadecyldimethyl[3-trimethoxysilyl]-propyl]ammonium chloride.<sup>2</sup>

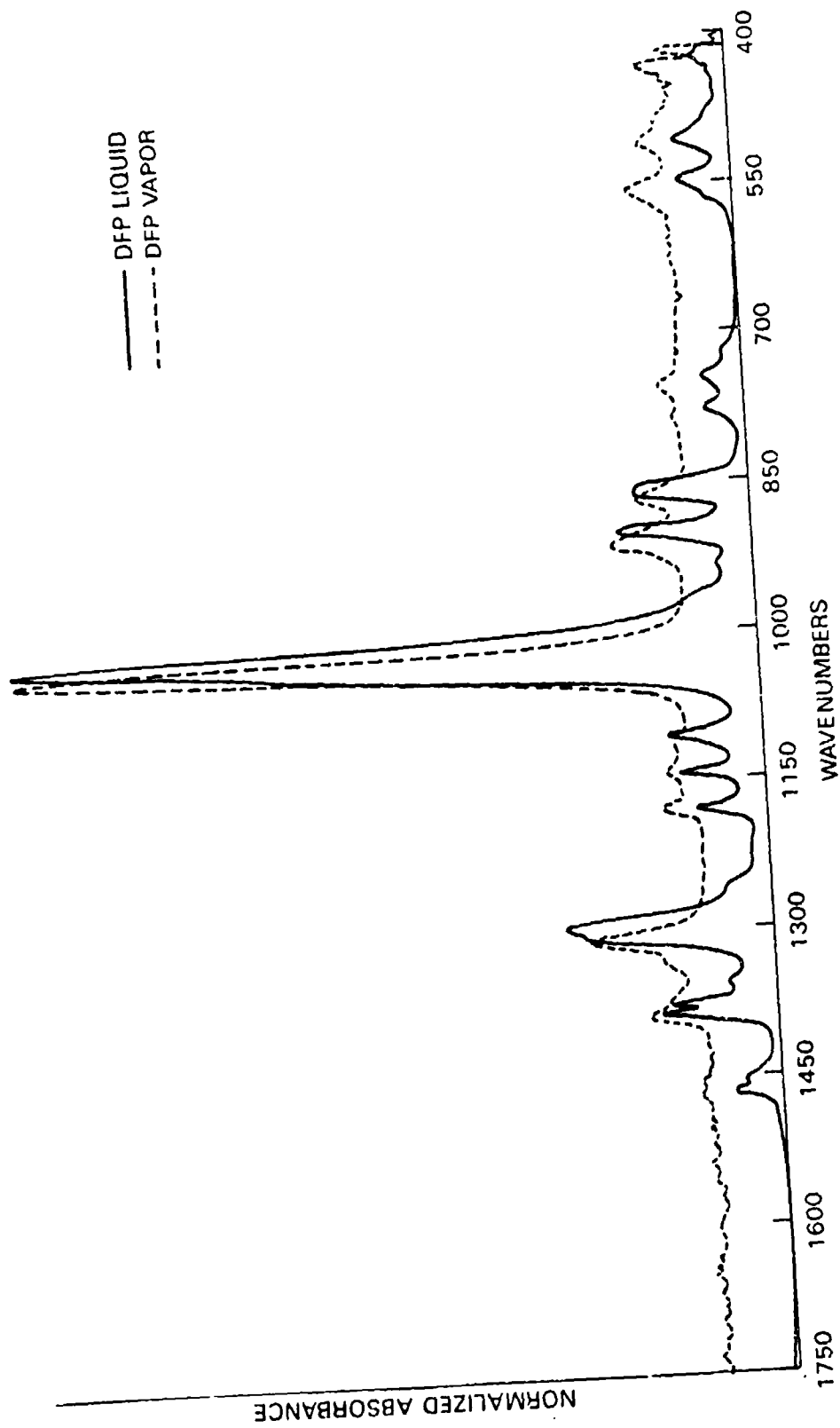
TABLE III. Vibrational Frequencies ( $\text{cm}^{-1}$ ) of Final Adsorption/Reaction Species of DFP on Strem Silica and Woelm Alumina.

Silica	Assignment	Alumina
2987		2982
2942		2937
2881		2882
1467		1469
1457		1454
1391		1388
1382		1377
1357(vw)		---
1279	Subtraction artifact from a silica band	---
1257(sh)	$\nu(\text{P}=\text{O})$	---
1180(w)		1210
1139(w)	$\nu(\text{Al-F}) \approx 1140(\text{br})$	1180(m) 1143(vw) 1109(vw) 1082(m)
1103(w)		
1026	$\nu(\text{P-O-C})$	1011
950(sh)		
917	due to subtraction of silica band	
900(sh)	$\text{CH}_3$ rock	
874	$\nu(\text{P-F})$ appears at higher frequency due to oversubtraction of silica band	
790		
750		
737		
565		poor S/N below
529		900 $\text{cm}^{-1}$ due to
500		strong $\text{Al}_2\text{O}_3$ band

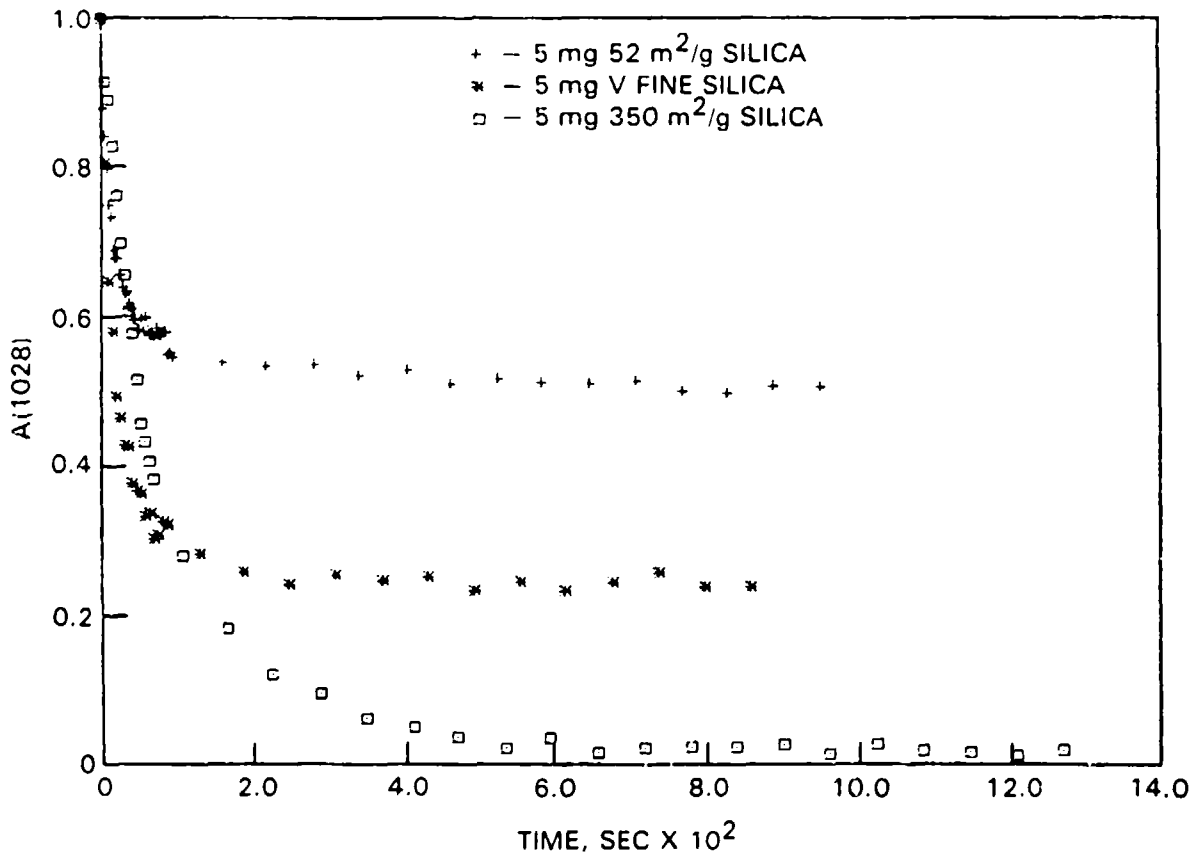
## FIGURE CAPTIONS

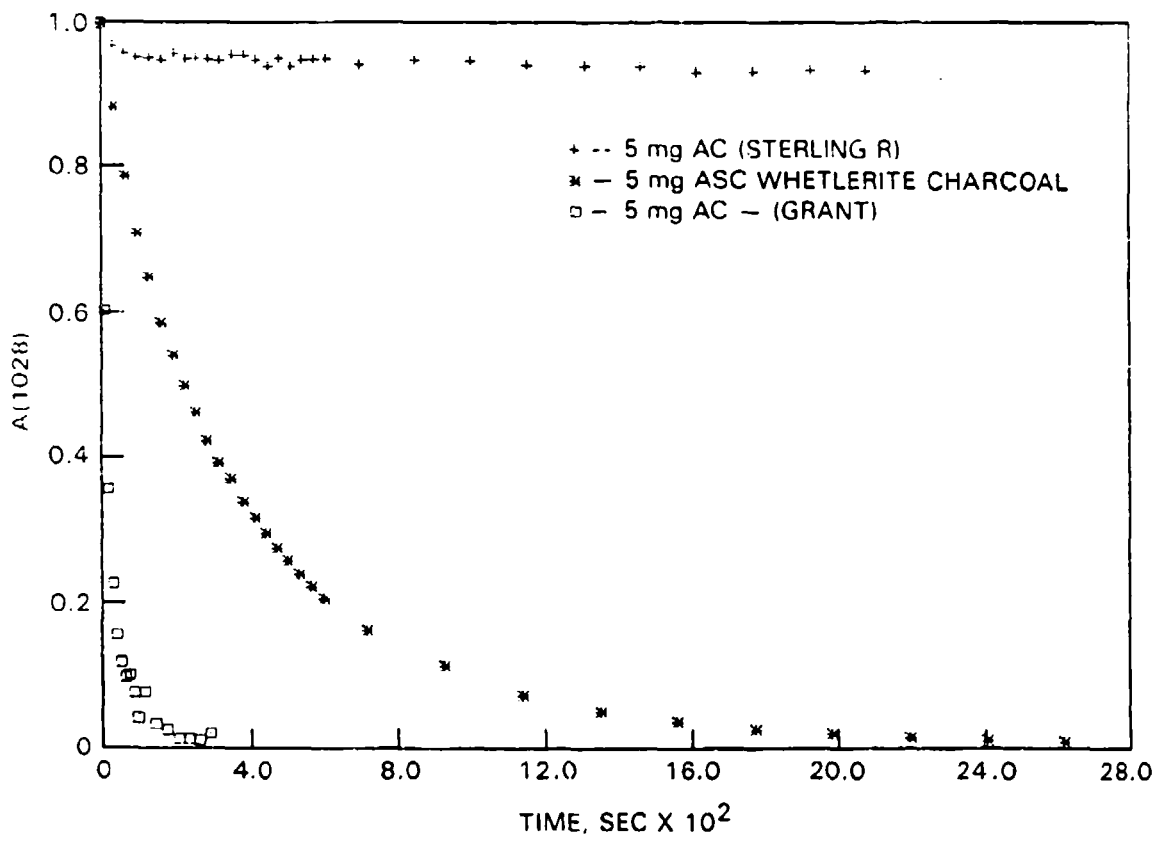
1. Gaseous and Liquid DFP IR Spectra.
2. DFP Adsorption on Three Different Surface Area Silicas.
3. DFP Adsorption Rate on Three Different Charcoals.
4. DFP/N<sub>2</sub> Flow System.
5. Absorbance (1028 cm<sup>-1</sup>) Versus Time Plot at P/P<sub>0</sub> = 0.67 DFP on 350 m<sup>2</sup>/g Strem Silica.
6. Adsorption Isotherm (24 ± 2°C) for DFP on 350 m<sup>2</sup>/g Strem Silica.
7. Adsorption Isotherm (24 ± 2°C) for DFP and DFP + H<sub>2</sub>O on SiEDA Silica.
8. N<sub>2</sub> Desorption of DFP From Silica, SiEDA Silica, and Walls.
9. GC Reconstruction of DFP Adsorption onto Woelm Alumina Showing DFP, H<sub>2</sub>O, CO<sub>2</sub>, and IPA Retention.
10. DRIFT Spectra of DFP + H<sub>2</sub>O on Strem Silica and Woelm Alumina Compared to Liquid DFP Spectrum.

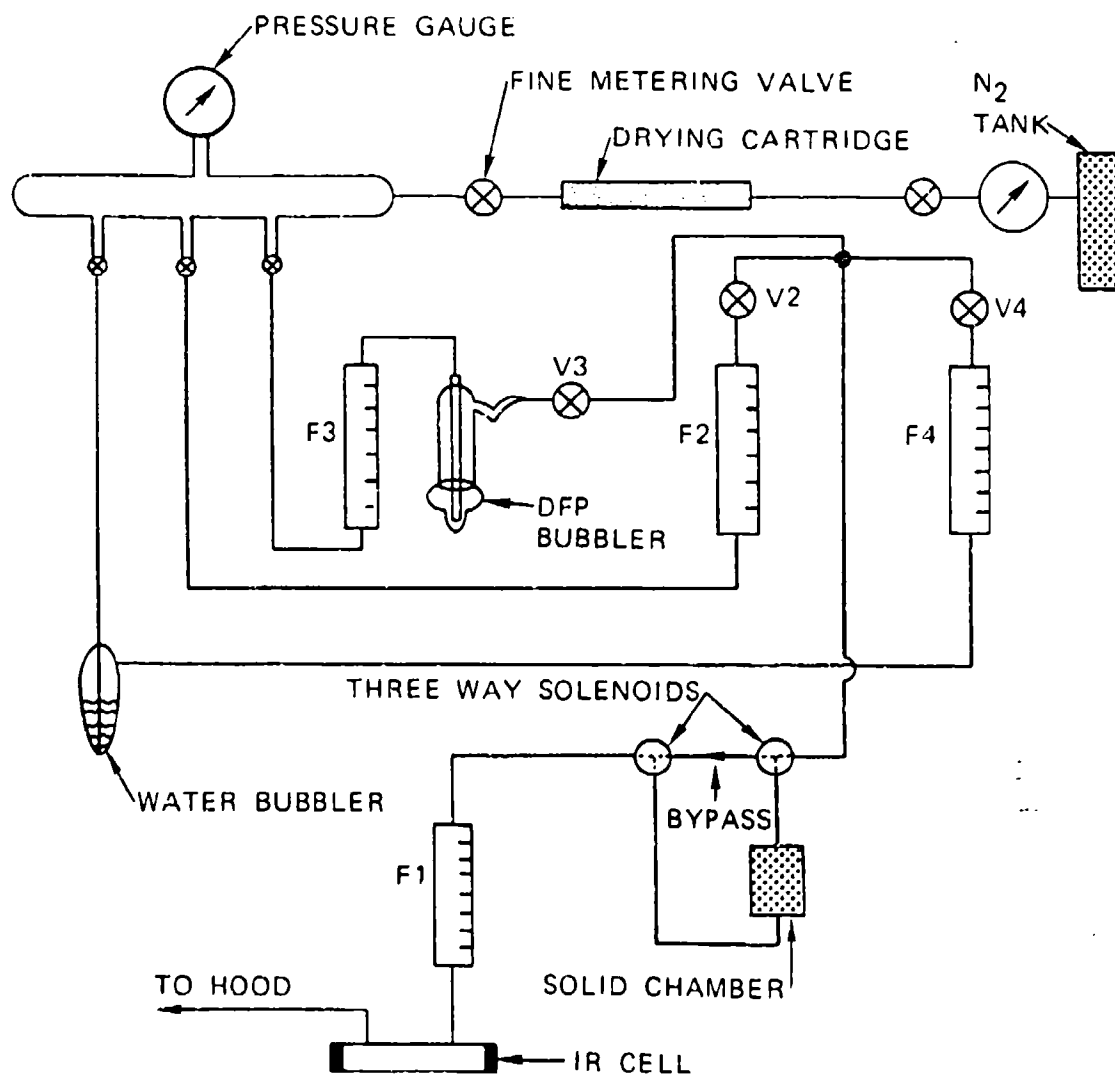
11. PA Spectra of Initial (a) and Final (b) Species From DFP(g) + Alcoa CSS350 Alumina Reaction.
12. Hydrolysis Rate of DFP(g) on CSS350 and F200 Alcoa Alumina.
13. Solid State  $^{31}\text{P}$  NMR of DFP( $\ell$ ) on Silica.
14. Solid State  $^{31}\text{P}$  NMR of (a) DFP( $\ell$ ) on SiQOCT and (b) DFP + H<sub>2</sub>O on SiQOCT.
15. Solid State  $^{31}\text{P}$  NMR of DFP( $\ell$ ) on Whetlerite Activated Charcoal.

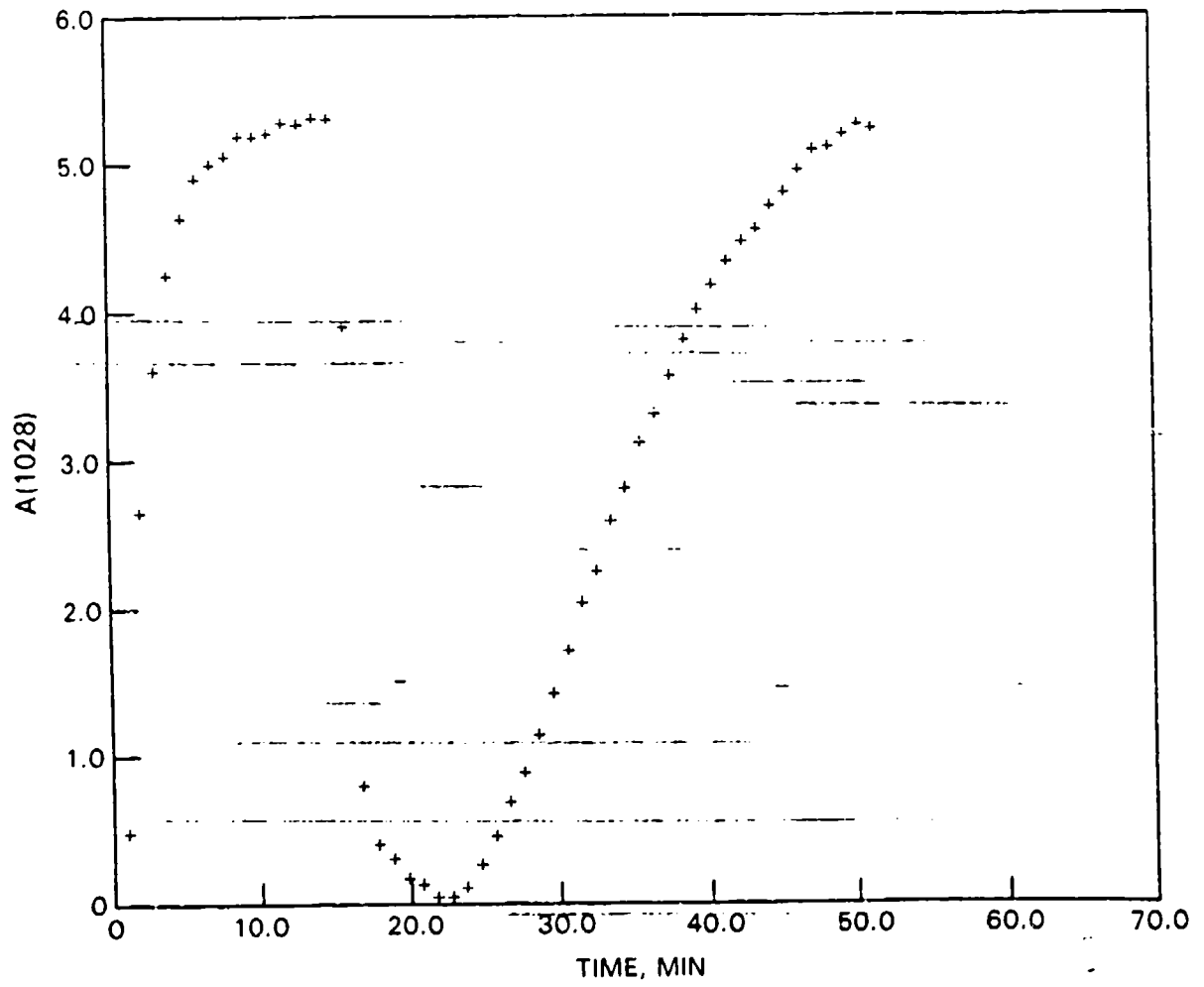


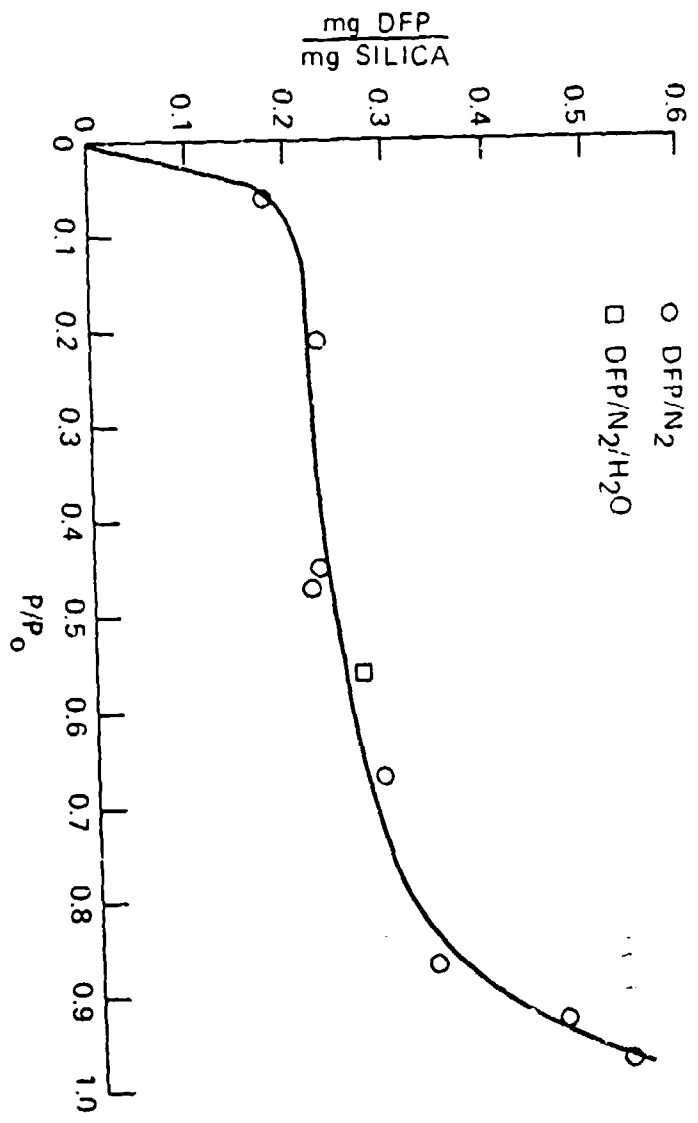
— DFP LIQUID  
- - - DFP VAPOR

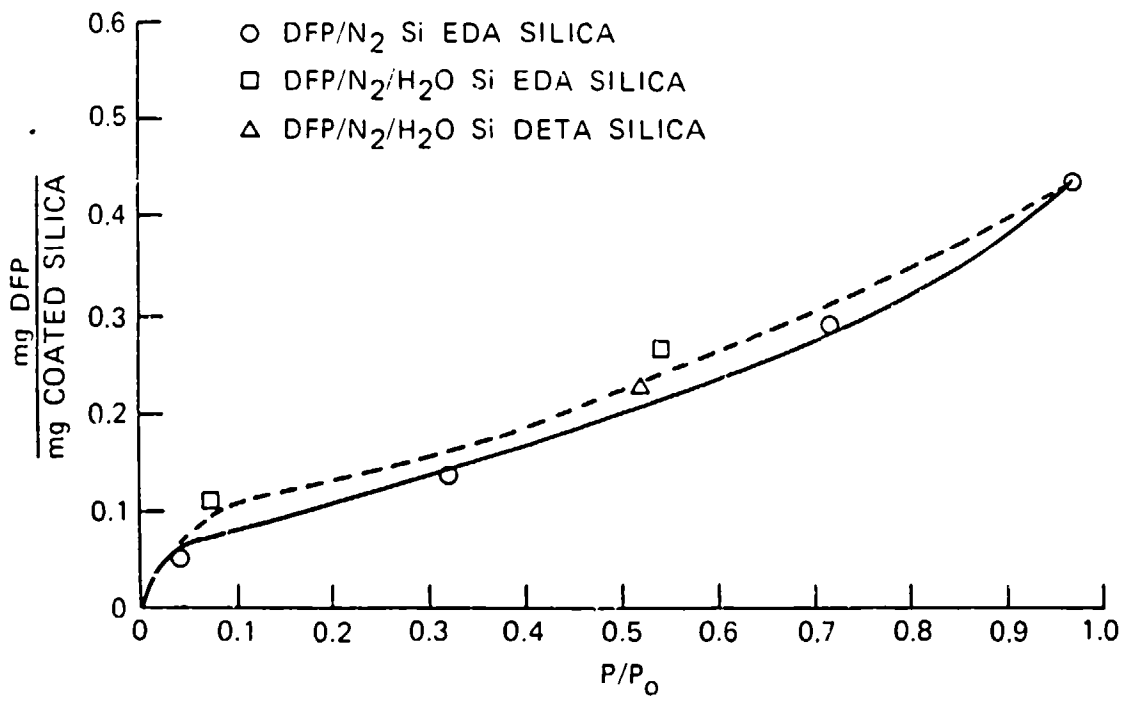


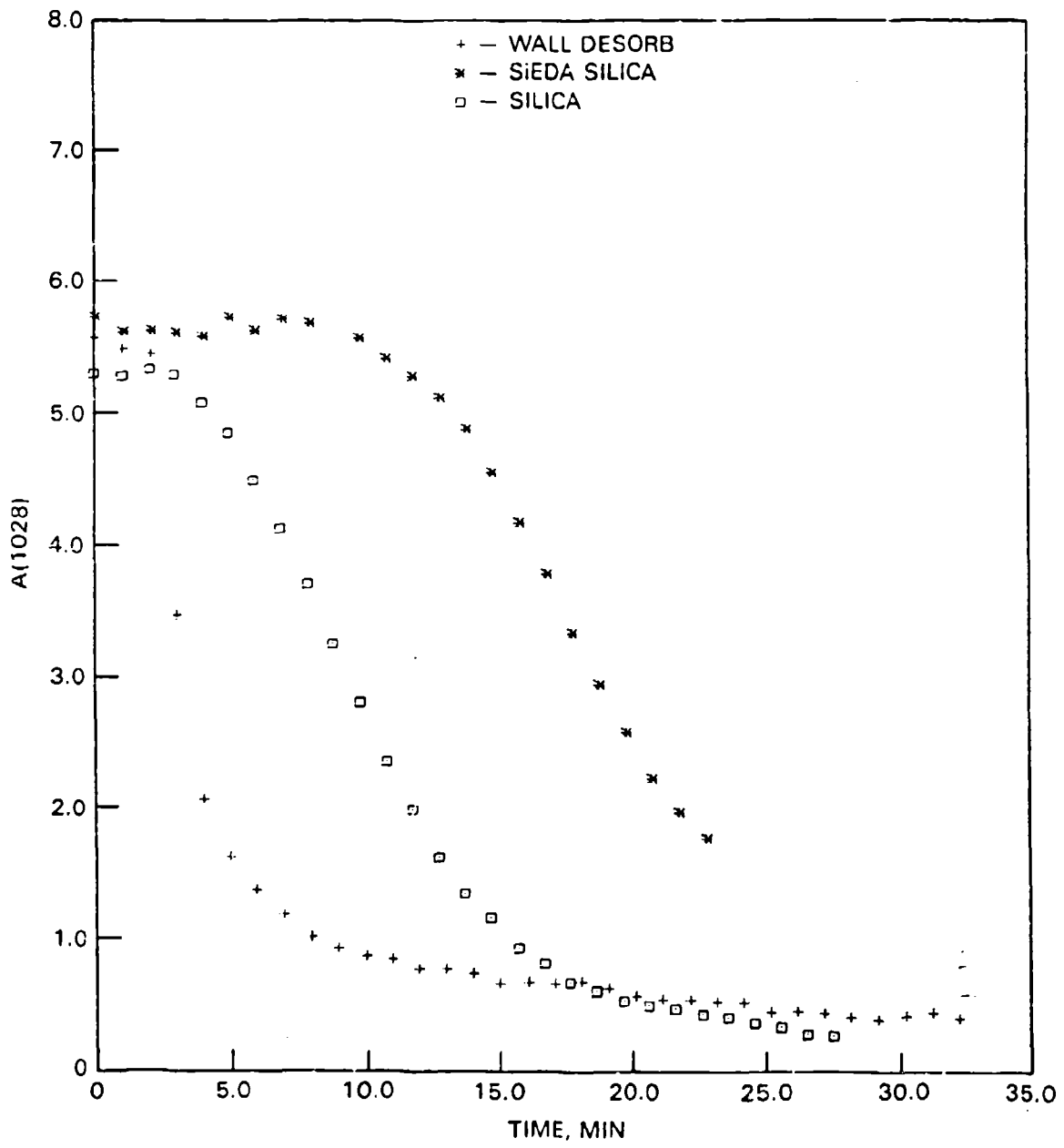


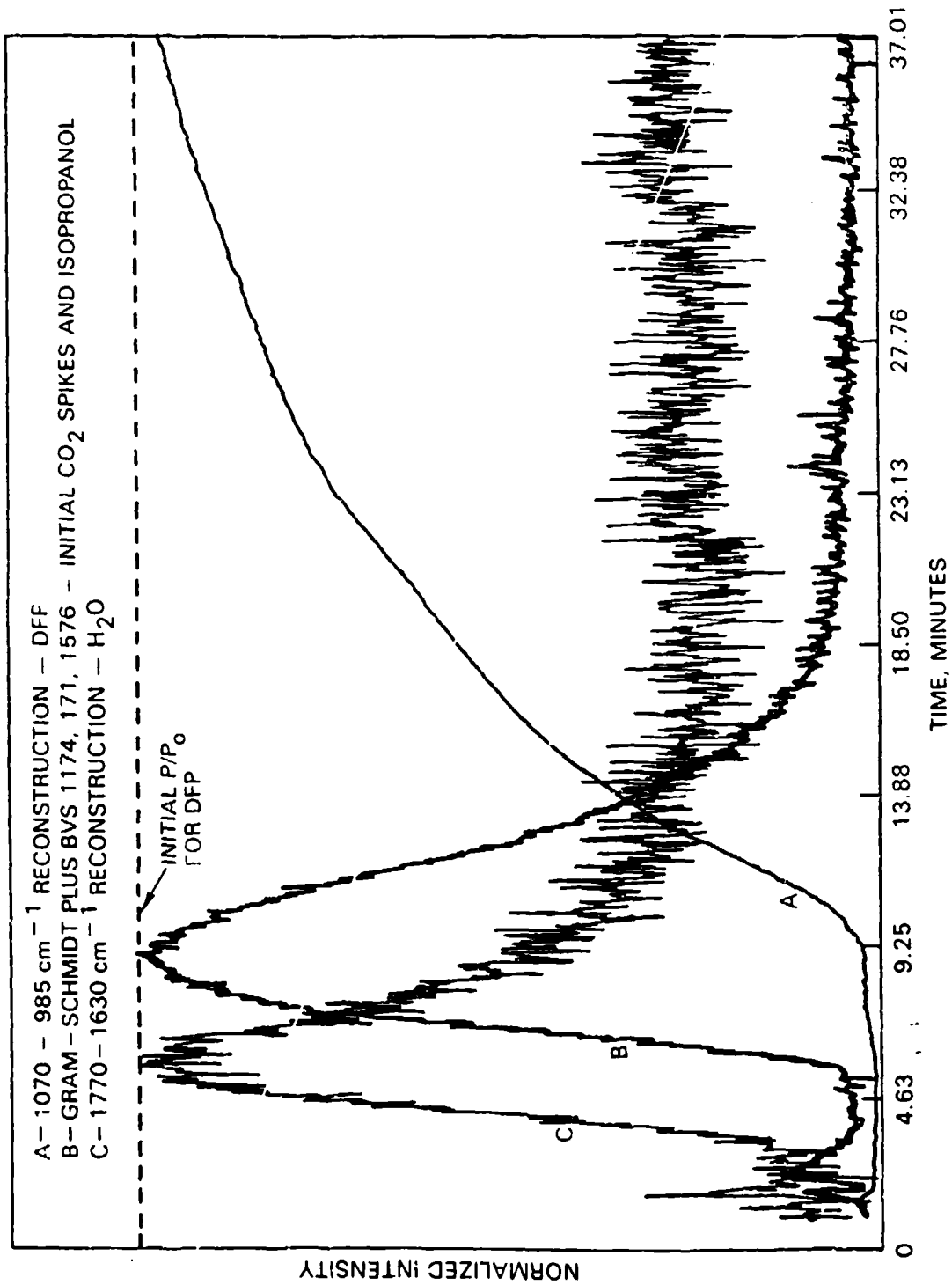




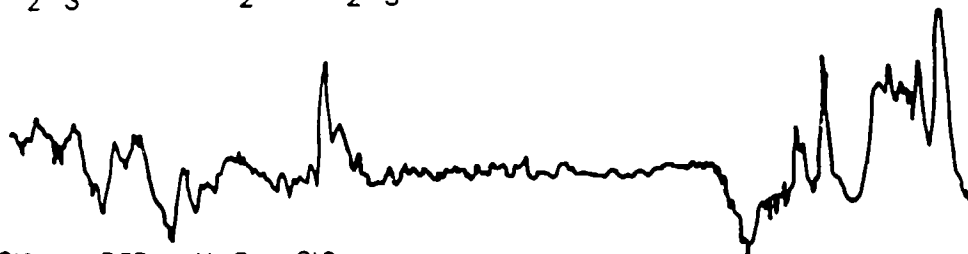








$\text{Al}_2\text{O}_3 + \text{DFP} + \text{H}_2\text{O} - \text{Al}_2\text{O}_3$



$\text{SiO}_2 + \text{DFP} + \text{H}_2\text{O} - \text{SiO}_2$



LIQUID DFP

